

Probing Dark Energy with Precise and Accurate Weak Lensing from Joint Ground- and Space- Based Imaging

Applicant/Institution:	Brookhaven National Laboratory
Street Address/City/State/Zip:	Building 510, Upton, NY 11973
Postal Address:	P.O. Box 5000, Upton, NY 11973
Principal Investigator (PI) name, telephone number and email:	Xiangchong Li, 412-527-0597 xli6@bnl.gov
Administrative Point of Contact name, phone, email:	Rolf Lageraaen, 631-344-2301 rlageraaen@bnl.gov
NOFO Number:	DE-FOA-0003602
DOE/SC Program Office (ASCR, BER, BES, FES, HEP, NP, DOE IP):	HEP
Research area or areas as identified in Section III of this NOFO:	Experimental Research at the Cosmic Frontier of High Energy Physics
DOE/SC Program Office Technical Contact:	Bryan Field Bryan.Field@science.doe.gov
Year Doctorate Awarded:	2021
Number of Times Previously Applied:	0
PAMS Preapplication tracking number:	0000048223
Application Contains Data Management Plan in Appendix 4: (Yes or No)?	Yes

Project Summary/Abstract

Probing Dark Energy with Precise and Accurate Weak Lensing from Joint Ground- and Space-Based Imaging

Xiangchong Li | Brookhaven National Laboratory

Understanding the physical origin of cosmic acceleration is one of the central open questions of the Cosmic Frontier, and Stage-IV weak lensing was identified by the Snowmass and P5 processes as a top priority for the coming decade. This single-investigator project (PI: Xiangchong Li, Brookhaven National Laboratory) will deliver, for the first time at survey scale, an end-to-end joint weak-lensing analysis for the Vera C. Rubin Observatory's Legacy Survey of Space and Time (LSST) and the Euclid space telescope—a joint pixel-level image-processing pipeline coupled to a Gaussian-prior field-level cosmology inference framework—and apply it to sharpen LSST's constraints on whether dark energy is dynamical, i.e. whether its equation of state, $w(a) = w_0 + w_a(1 - a)$, departs from a cosmological constant. The **scientific merit** is a substantial gain in weak-lensing constraining power: joint pixel-level detection raises the LSST weak-lensing effective galaxy number density by at least $\sim 50\%$, AI-based shape estimation reduces the per-galaxy shape noise by an additional 10–20%, and Euclid near-infrared photometry reduces the catastrophic photometric-redshift outlier rate by 25–40% at $z \gtrsim 1$ —together conservatively delivering at least a 25% improvement in the LSST weak-lensing two-point constraint on dynamical dark energy and an independent test of the recent DESI-motivated hint of time-evolving dark energy. The **technical merit** is twofold: a fast, analytical, AI-compatible shear-calibration framework that removes the dominant systematic bottleneck for joint multi-survey imaging, and a tractable Gaussian-prior field-level inference pipeline for the joint catalog, built to be extended to a full field-level analysis that extracts non-Gaussian information with non-Gaussian priors from cosmological simulations.

This program takes advantage of the synergy between Rubin LSST—in which DOE has made a major investment, including LSSTCam—and the Euclid space mission, extracting substantially more dark-energy science from existing observational and computational resources at no additional hardware cost. Its physics-informed AI methods for shear estimation also advance the goals of the DOE Genesis Mission to accelerate scientific discovery with artificial intelligence. The infrastructure developed here will help enable Rubin LSST to deliver the robust dark-energy constraints it was built to provide, and is designed to extend naturally to a joint LSST×Euclid×Roman analysis.

The program is organized around **four coupled thrusts**: (#1) a joint LSST×Euclid image-processing pipeline (joint detection, AI-based shear estimation with chromatic-PSF correction, and joint flux and photo- z); (#2) a Gaussian-prior field-level cosmology analysis pipeline; (#3) a pathfinder analysis on the $\sim 1,000 \text{ deg}^2$ overlap between Euclid DR1 and the Dark Energy Survey (DES), a wide-area precursor survey to LSST; and (#4) deployment on the $> 3,000 \text{ deg}^2$ LSST-DR1×Euclid-DR2 overlap, supported throughout by a dedicated overlapped ground–space image-simulation suite for sub-percent shear calibration. The PI is exceptionally well positioned to open this exciting new area: the program builds on the PI's mature, validated AnaCal analytical shear-calibration framework rather than starting from scratch, and validates the full chain on a pathfinder dataset before production. The PI developed AnaCal from first principles, led the Year-3 image-simulation campaign, shear catalog, and cosmic-shear analysis of the Subaru Hyper Suprime-Cam (HSC) survey, the deepest precursor survey to LSST, and produced the LSST Commissioning Camera Data Preview 1 AnaCal shear catalog. Brookhaven National Laboratory provides the high-performance computing and the LSST Dark Energy Science Collaboration institutional context required, and Laboratory Directed Research and Development funding de-risks the AI components ahead of the program.

Table of Contents

PROJECT NARRATIVE	1
1 Background and Objectives	1
Dark Energy and Cosmic Acceleration	1
Weak Lensing with Stage-IV Surveys	2
AnaCal: Robust and Efficient Shear Estimation	3
Physics-Informed AI Shear Estimation with AnaCal	6
Toward Field-Level Inference for Joint Stage-IV Imaging	6
2 Scientific and Technical Merit	7
Scientific Merit	7
Technical Merit	8
3 Proposed Research and Methods	9
Thrust #1: Joint LSST×Euclid image processing	10
Thrust #2: Field-level cosmology analysis	10
Thrust #3: DES×Euclid-DR1 pathfinder analysis	11
Thrust #4: LSST-DR1×Euclid-DR2 analysis	11
4 Timetable of Activities	11
Contingencies and Risk Mitigation	13
5 Competency of Applicant’s Personnel and Adequacy of Proposed Resources	14
6 Potential For Leadership Within the Scientific Community	15
APPENDIX 1: Bibliography & References	16
APPENDIX 2: Facilities & Other Resources	21
APPENDIX 3: Equipment	22
APPENDIX 4: Data Management Plan	23
APPENDIX 5: Synergistic Activities	24
APPENDIX 6: Transparency of Foreign Connections	25
APPENDIX 7: Other Attachments	26

PROJECT NARRATIVE

1 Background and Objectives

Dark Energy and Cosmic Acceleration

Understanding the physical origin of **cosmic acceleration** is one of the central open questions in modern cosmology. In the standard Λ CDM model, this acceleration is attributed to **dark energy** in the form of a cosmological constant, Λ , whose energy density remains constant as the Universe expands. A more general possibility is that dark energy is dynamical, with an equation of state that evolves with cosmic time. This evolution is commonly parameterized as [1]

$$w(a) = w_0 + w_a(1 - a), \quad (1)$$

where a is the cosmic scale factor ($a = 1$ today), $w(a)$ is the ratio of dark-energy pressure to density, w_0 is its present-day value, and w_a describes its time evolution. A cosmological constant corresponds to $w_0 = -1$ and $w_a = 0$; a statistically significant departure would indicate physics beyond the standard cosmological model. The U.S. Department of Energy (DOE) has invested heavily in the Vera C. Rubin Observatory's Legacy Survey of Space and Time (LSST) [2] and the Dark Energy Spectroscopic Instrument (DESI) [3] to probe whether $w(a)$ deviates from a cosmological constant.

DESI is mapping tens of millions of galaxy and quasar redshifts over $\sim 14,000 \text{ deg}^2$ to trace baryon acoustic oscillations (BAO) [4] and structure growth. The DESI Data Release 2 (DR2) BAO analysis provides the most precise BAO measurements to date [5, 6]; combined with cosmic microwave background (CMB) and Type Ia supernova datasets, they show $3\text{--}4\sigma$ evidence that dark energy may evolve with time [7]. Since this hint is driven by BAO distances combined with external CMB and supernova datasets, establishing whether dark energy truly evolves demands an independent probe with different parameter degeneracies and dominant systematics.

Weak gravitational lensing (WL) [8] is precisely such a probe: by measuring the coherent distortions of galaxy images caused by foreground matter, WL is sensitive not only to geometry but also to the structure growth, providing exactly the information needed to deliver an independent test of the DESI-motivated hint of dynamical dark energy. Delivering this test is one of the central dark-energy science goals of Rubin LSST.

A robust WL confirmation of a time-evolving dark-energy equation of state with the DOE's Rubin LSST would mark one of the most important breakthroughs in cosmology in more than a decade. **This proposal combines LSST and Euclid [9] imaging at the pixel level for the first time at survey scale**, via four coupled thrusts: (#1) a joint LSST \times Euclid image-processing pipeline (joint detection, artificial-intelligence (AI) shear estimation with chromatic point-spread-function (PSF) correction, joint flux and photo- z); (#2) a Gaussian-prior field-level cosmology pipeline on the resulting catalog; (#3) a Dark Energy Survey (DES) \times Euclid-DR1 pathfinder on the $\sim 1,000 \text{ deg}^2$ overlap (FY27–FY28); and (#4) the first LSST-DR1 \times Euclid-DR2 joint WL dark-energy analysis on the $> 3,000 \text{ deg}^2$ overlap (FY29–FY31). Joint pixel-level detection raises LSST WL n_{eff} by at least $\sim 50\%$ [10, 11]; AI-based shape estimation [12, 13] cuts per-galaxy shape noise by an additional 10–20%; and Euclid near-infrared (NIR) photometry reduces catastrophic photo- z outliers by 25–40% at $z \gtrsim 1$ [14, 15]. Together, these advances conservatively deliver at least a 25% improvement in the LSST WL constraint on dark energy, providing an independent test of the DESI-motivated hint.

Weak Gravitational Lensing with Stage-IV Surveys

The next five years will mark a golden age for weak-lensing cosmology. Data from the Stage-IV imaging surveys—Rubin LSST, Euclid, and the Nancy Grace Roman Space Telescope (Roman) [16]—are arriving in close succession, and **joint pixel-level processing** of Rubin LSST and Euclid is already recognized as an immediate priority for Stage-IV dark-energy science. The simultaneous rapid development of **artificial intelligence** technologies, together with the emergence of **field-level** weak-lensing inference that forward-models the survey footprint directly, further amplifies what a joint analysis of these surveys can deliver. Realizing this opportunity, however, hinges on a technical bottleneck in **shear calibration**: the complicated procedure required to meet the LSST Dark Energy Science Collaboration (DESC) sub-percent multiplicative-bias requirement, together with the large computational cost of the joint multi-survey image processing and the overlapped simulation campaigns needed to validate and calibrate it. To remove this bottleneck, in the next subsection we propose a fast and simple analytical shear-estimation framework that is compatible with AI by design.

WL is the small, coherent distortion (“shear”) of distant galaxy images by the intervening matter distribution along the line of sight [17–20], and is measured statistically across very large galaxy populations because the per-galaxy signal is more than an order of magnitude smaller than the intrinsic shape variation. Dark energy affects WL both by altering the distance–redshift relation that sets lensing efficiency and by suppressing the late-time growth of cosmic structure that sets the amplitude of WL correlations, so WL surveys probe cosmic geometry and structure growth simultaneously, complementing the BAO distance ladder of DESI. Equally important, the dominant WL systematics—shear estimation bias, PSF modeling, galaxy blending, intrinsic alignments, and photometric-redshift errors—are largely orthogonal to those of spectroscopic BAO, making WL the decisive independent probe with which to test the DESI-motivated hint of dynamical dark energy. The pioneering Stage-III imaging surveys—DES [21], Hyper Suprime-Cam (HSC) [22], and the Kilo-Degree Survey (KiDS) [23]—have established the modern cosmic-shear methodology and produced precise measurements of the structure-growth amplitude

$$S_8 \equiv \sigma_8 \sqrt{\Omega_m/0.3}, \quad (2)$$

finding values $0.5\text{--}2.5\sigma$ below the *Planck* CMB [24] value under Λ CDM. With substantially larger area, greater depth, improved redshift information, and tighter control of shear systematics, the Stage-IV imaging surveys—now operating or coming online over the next few years (Figure 1)—will transform this emerging “ S_8 tension” into a high-precision measurement of structure growth and an independent test of the DESI-motivated hint of dynamical dark energy. Among the LSST cosmological probes, WL $3\times 2pt$ is forecast to deliver the tightest single-probe constraint on the dark-energy equation-of-state parameters w_0 and w_a (Figure 2).

The scientific case for joint LSST–Euclid weak-lensing analysis is well established. Catalog-level forecasts show that combining LSST and Euclid shape measurements of the same galaxies increases the effective galaxy number density n_{eff} of the LSST WL sample by $\sim 50\%$ [10], and pixel-level joint detection and shape measurement—the approach pursued here—is expected to deliver still larger gains, as identified by the 2020 Joint Survey Processing Study Group [11]. Physics-informed AI shape estimators (D_4 -equivariant convolutional neural networks [CNNs] trained with denoising score matching) [12, 13] further reduce the per-galaxy shape noise by an additional 10–20% on top of this joint-detection n_{eff} gain. Joint processing also tightens the photometric redshifts that underpin tomographic WL: adding Euclid NIR photometry to LSST *ugrizy* imaging reduces the catastrophic-outlier rate by 25–40%, especially at $z \gtrsim 1$, where 4000 Å-break/Lyman-break confusion makes optical colors degenerate [14, 15]. Both gains arise from the same complementarity—LSST contributes optical depth and multi-band sampling, Euclid contributes space-based resolution and NIR coverage—and pixel-level forced photometry across the two surveys yields consistent

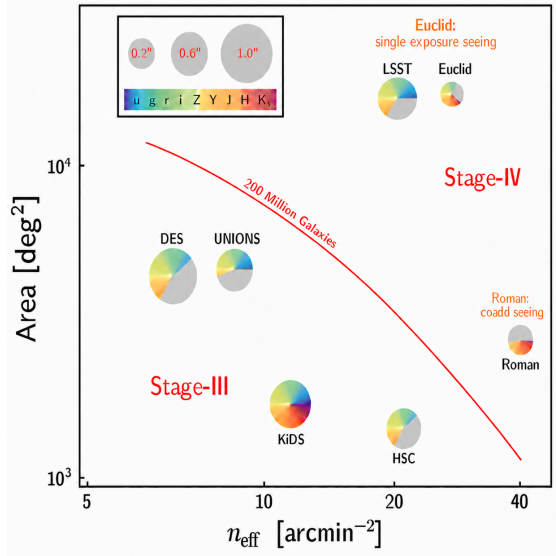


Figure 1: The Stage-III and Stage-IV imaging surveys. The diameter of each disk represents the size of the point-spread function (PSF) of the corresponding survey, and the color encodes its wavelength coverage from the ultraviolet (u band) to the near-infrared (K band).

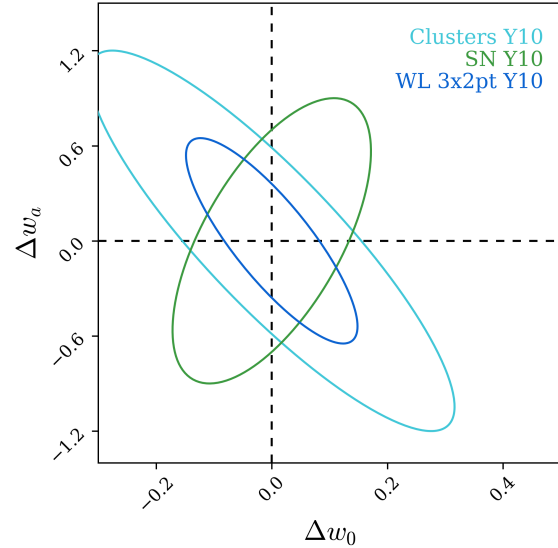


Figure 2: Forecast LSST ten-year 68% constraints on Δw_0 , Δw_a from WL $3 \times 2pt$ (blue), Type Ia SNe (green), and clusters (cyan). WL gives the tightest individual constraint and is the focus of this proposal. Adapted from Fig. G2 of the LSST DESC Science Requirements Document [25].

u -through- H flux measurements for the same sources, avoiding catalog-matching ambiguities that limit existing multi-survey combinations and enabling consistent detection bias correction in shear estimation. Figure 3 illustrates this multi-band, multi-resolution complementarity in joint imaging of an eRASS1 galaxy cluster across Rubin, DES, and Euclid. These gains make pixel-level LSST–Euclid joint processing an immediate priority for Stage-IV dark-energy science, also recognized by the Astro2020 Decadal Survey white paper [26], and the pipeline developed here will extend naturally to Roman once Roman coadd imaging products are released.

Realizing this opportunity, however, hinges on meeting the LSST DESC sub-percent shear-calibration requirement [25] at survey scale on heterogeneous data. Classic high-accuracy shear calibration applies small artificial shears to the images and reruns the full measurement chain on each sheared realization to capture detection and selection biases at the sub-percent level. This chain is intricate to validate and computationally demanding for joint-survey analysis, and remains the principal obstacle to turning the long-recognized promise of joint ground–space weak-lensing analysis into an operational survey-scale pipeline.

AnaCal: Robust and Efficient Self Calibration for Shear Estimation

This proposal develops a survey-scale joint-imaging shear estimator for combined ground- and space-based data, closing the gap identified above: the absence of a method that can meet the LSST DESC sub-percent shear-calibration requirement at affordable cost. The work extends the PI’s **AnaCal** [28, 29] framework into a joint ground–space pipeline for Stage-IV weak lensing. AnaCal computes the shear response in closed form and propagates it by automatic differentiation, eliminating the four counterfactual image-shearing realizations of Metacalibration/Metadetection and cutting shear-catalog production cost by $\sim 100\times$ at sur-

vey scale—bringing LSST×Euclid joint-imaging catalog production within reach on standard LSST DESC compute, and supplying the analytic gradients that make downstream gradient-based field-level cosmology inference tractable. The same differentiable construction makes AnaCal AI-compatible by design, supporting model-fitting features and symmetry-equivariant neural feature extractors within a single self-calibrated pipeline.

Shear-estimation accuracy is summarized by $g_{\text{obs}} = (1 + m)g_{\text{true}} + c$ [30, 31], where m is the multiplicative bias and c the additive bias; the LSST DESC SRD requires $|m| < 0.3\%$ across redshift bins [25]. *Perturbative* self-calibrating estimators (Metadetection and AnaCal) already achieve this target even on heavily blended images by expanding the measured ellipticity e to first order in the applied shear g and exploiting the spin-2 symmetry of weak lensing:

$$\langle e \rangle = \langle e_0 \rangle + g \left\langle \frac{\partial e}{\partial g} \right\rangle + g^2 \left\langle \frac{\partial^2 e}{2\partial g^2} \right\rangle + \mathcal{O}(g^3). \quad (3)$$

Under isotropically distributed galaxy orientations, both $\langle e_0 \rangle$ (spin-2) and the second-order contribution (spin-2 plus spin-6) vanish, leaving only the spin-0 mean shear response $\langle \partial e / \partial g \rangle$. **Metacalibration** [32, 33] and **Metadetection** [34] estimate this response *numerically*, by finite-differencing measured shapes across image realizations with small artificial shears applied. This approach delivers part-per-thousand accuracy and underpins the DES Y6 shear catalog ($|m| < 0.3\%$), but at the cost of additional computational complexity: four extra sheared image realizations must be generated and processed.

AnaCal, by contrast, computes the analytical shear response for each smoothed image pixel and propagates it forward through detection, deblending, and measurement to the final observables [35], while noise-induced bias is corrected analytically using the symmetry of the noise field. Automatic differentiation through this construction yields a fully differentiable estimator that enforces the spin-2 symmetry of

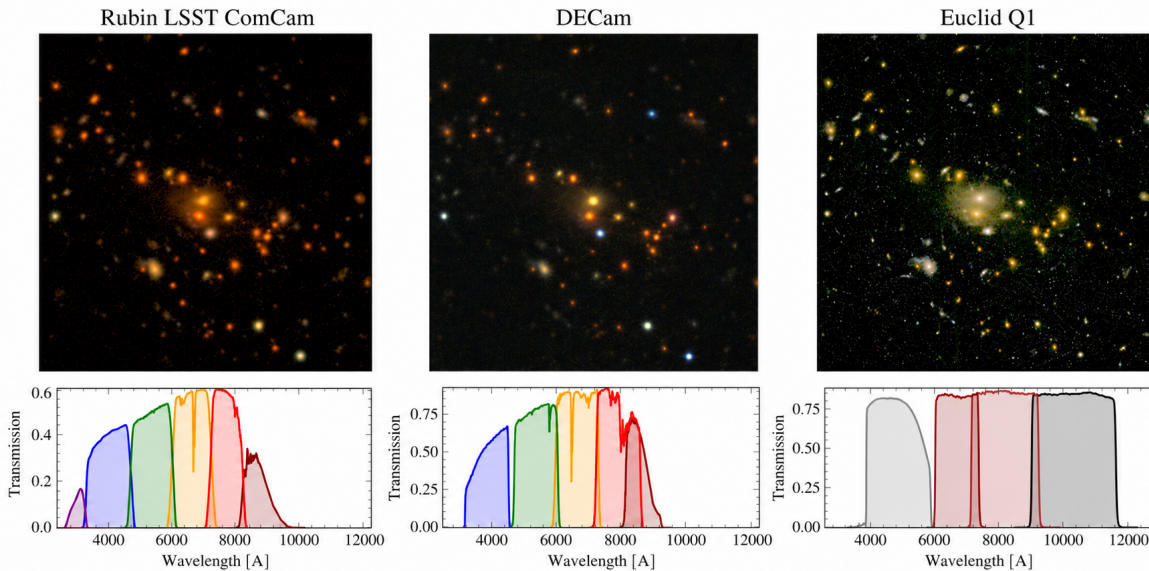


Figure 3: *Top*: Rubin Commissioning Camera Data Preview 1 (DP1), DES, and Euclid Quick Release 1 imaging of the same eRASS1 galaxy cluster [27] ($z = 0.69$, EDF-S). *Bottom*: corresponding filter transmission curves: Rubin *ugrizy*, DES *grizy*, and Euclid Visible Imager (VIS) plus Near-Infrared Spectrometer and Photometer (NISP; *Y, J, H*). The three surveys differ in depth, resolution, and wavelength coverage; joint pixel-level analysis across them underpins this proposal.

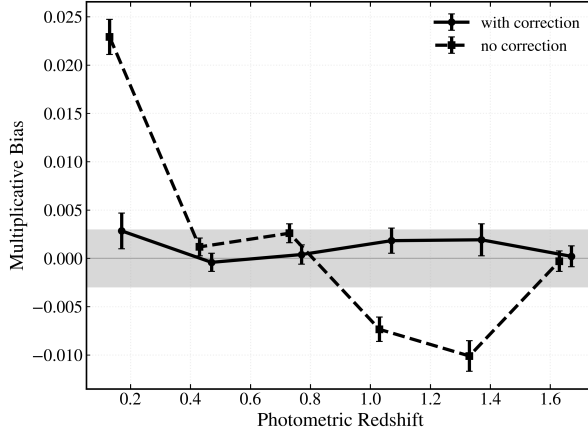


Figure 4: Multiplicative shear bias m as a function of FlexZBoost photometric redshift on LSST ten-year-like image simulations with blending. The *solid* line includes the analytical self-calibration for the selection bias induced by binning galaxies into tomographic redshift bins; the *dashed* line is without that correction. The *grey band* marks the LSST DESC requirement [25].

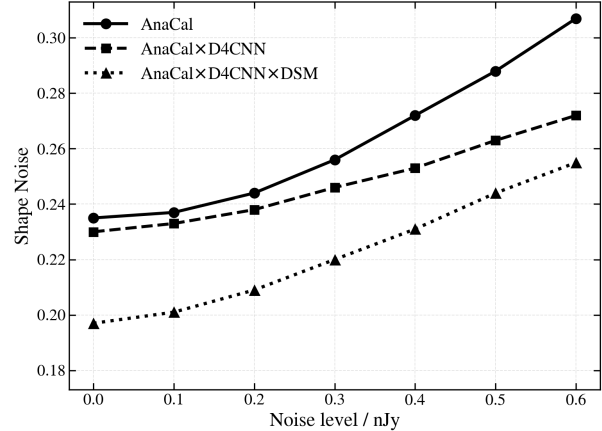


Figure 5: Per-component galaxy shape noise as a function of pixel-noise standard deviation σ_{noise} on LSST-like image simulations. *Solid*: AnaCal alone; *dashed*: AnaCal combined with a D₄-equivariant CNN [12]; *dotted*: AnaCal + D₄CNN further optimized with denoising-score matching. The expected LSST Year-10 *i*-band noise level is $\sigma_{\text{noise}} = 0.59$.

Survey	Method	Area [deg ²]	n_{eff} [arcmin ⁻²]	z range	$\sigma(S_8)$
DES Y6	Metadetection	$\sim 4,200$	~ 8.2	0.3–1.5	~ 0.015
HSC Y6	AnaCal	~ 800	~ 15	0.3–1.5	~ 0.019

Table 1: Footprint, effective source density, source-redshift range, and measured uncertainty on S_8 for the Stage-III cosmic-shear analyses. The DES Y6 entry is the forecast for the final DES analysis. HSC Y6 refers to the HSC-SSP collaboration’s internal Year-6 dataset (*not* unblinded and published yet); the corresponding cosmic-shear analysis is currently unpublished and blinded, and final published values may differ slightly from those quoted here.

weak lensing, suppresses the leading second-order bias terms (Equation (3)), and achieves $|m| < 0.3\%$ across all redshift bins. Because the shear response is evaluated analytically rather than by finite-differencing four artificially sheared image realizations, AnaCal cuts shear-catalog production cost by $\sim 100\times$ at survey scale, and the same analytic gradients feed directly into the downstream gradient-based field-level cosmology inference (Thrust #2) at negligible additional compute. Figure 4 demonstrates this on LSST Y10 image simulations, with photo- z estimated using FlexZBoost [36] in the RAIL [37] framework: the solid curve includes AnaCal’s analytical self-calibration for tomographic-binning selection effects (without external simulations) and lies safely within the LSST DESC SRD band.

Avoiding the artificial-shearing step makes AnaCal $\sim 100\times$ faster than Metadetection: processing the full LSST *ugrizy* coadd at survey scale requires only $\sim 10^4$ CPU hours (a few hundred node-hours on the National Energy Research Scientific Computing Center [NERSC] Perlmutter). The same differentiable construction extends naturally to physics-informed AI shear estimation, propagating the shear response through machine-learned D₄-equivariant representations of galaxy images [12] while preserving analytical self-calibration.

AnaCal is already deployed at survey scale: it is the shear pipeline for the ongoing HSC Year-6 cosmology analysis (PI is a core contributor), has been run on LSST Commissioning Camera DP1 [38], is being extended to LSST Data Preview 2 (DP2), and has been validated for the chromatic-PSF effects [39] relevant to joint Rubin–Roman weak lensing [40, 41]. Table 1 compares the resulting HSC Y6 cosmic-shear analysis with DES Y6 in survey area, source density, redshift range, and S_8 uncertainty (Equation (2)).

Physics-Informed AI Shear Estimation with AnaCal

The fast, AI-compatible AnaCal pipeline is the natural foundation on which to build the next generation of shear estimators. Deep neural networks learn flexible pixel-level representations relevant to shape measurement, deblending, and multi-band galaxy morphology, going beyond hand-crafted moment features. **Physics-informed AI shear estimators**—neural networks acting as the feature extractor while the shear response is analytically propagated and calibrated through AnaCal—are therefore a natural extension: they reduce the per-galaxy shape noise by an additional 10–20% on top of the perturbative AnaCal baseline, while preserving the self-calibration needed for sub-percent shear-bias control.

The central technical challenge is that black-box ML shear estimators are not, on their own, calibratable to the LSST DESC sub-percent requirement [42, 43]: blindly trained networks introduce shape-dependent multiplicative bias at the 10^{-2} level, and simulation-based recalibration is prohibitive at survey scale. Two ingredients remove this obstacle. First, the analytical **AnaCal** calibration is applied to the network outputs by forward-propagating the analytical pixel-to-feature shear response through the trained network via automatic differentiation, which solves the shear-bias perturbation problem consistently through second order in g (Equation (3)). Second, a **D_4 -equivariant network** [44] embeds the D_4 group of 90° rotations and reflections into the network weights, so the predicted ellipticity transforms exactly as a spin-2 quantity under image rotations; this eliminates orientation-dependent biases and cuts the parameter count by $\sim 8\times$, yielding a $\sim 10\times$ training-data-efficiency gain at no accuracy cost.

A first realization of this $D_4\text{CNN} \times \text{AnaCal}$ architecture [12], demonstrated on isolated galaxies in LSST-like single-band simulations, achieves $|m| < 0.1\%$ **across all tested noise levels, PSF sizes and ellipticities, and magnitude cuts (most at the $\sim 10^{-4}$ level)**, while delivering $\sim 10\%$ lower shape noise than the moment-based estimator in the high-noise regime—equivalent to a $\sim 20\%$ gain in effective galaxy number density. A complementary advance, *denoising score matching* [13], trains the equivariant feature extractor to align with the analytical score function of the image likelihood (provably the minimum-variance unbiased shear estimator), reducing the per-component shape noise by another $\sim 10\%$ at LSST Y10 noise levels (Figure 5) while preserving $|m| < 0.1\%$ calibration.

Toward Field-Level Inference for Joint Stage-IV Imaging

The second methodological pillar of this proposal is enabling *field-level* weak-lensing inference on joint LSST \times Euclid data. Traditional two-point cosmic-shear analyses implicitly assume statistical homogeneity across the survey footprint, an assumption already violated within a single survey by depth and observing-condition variations [45], and broken much more severely when LSST-only, Euclid-only, and LSST–Euclid overlap regions are combined: these regions differ in depth, PSF, wavelength coverage, selection, and photo- z performance. Consequently, a two-point analysis can be applied to the joint mosaic only by partitioning it into approximately homogeneous sub-regions—the LSST \times Euclid overlap and the LSST-only and Euclid-only fields—and measuring the cosmic-shear correlations within each separately, since the sub-regions carry different redshift distributions $n(z)$ and shape noise; this piecemeal treatment neglects the cross-correlations between sub-regions, forfeiting cosmological information and degrading the dark-energy constraint below the optimum the joint data set can in principle deliver. Field-level inference instead forward-models these

spatially varying survey properties directly, letting the calibrated overlap anchor coherent inference across the larger non-overlapping footprints [46–50].

Current catalog-level cosmic-shear pipelines have no satisfactory way to handle this inhomogeneity: they either restrict the analysis to nominally homogeneous patches or absorb survey-property variations into approximate mode-coupling matrices, leaving residual systematics that threaten to become a dominant floor at Stage-IV precision [45]. The field-level pipeline *Miko*, developed by a student co-supervised by the PI [46], instead forward-models the analysis systematics (aliasing, boundary effects, mode coupling, density-induced shape noise) in pixel space, and has demonstrated on HSC Year-3-like mocks that this yields *unbiased* tomographic power-spectrum amplitudes under a Gaussian field-level prior, whereas a non-Gaussian log-normal prior introduces significant bias from prior misspecification. The proposed program therefore adopts the Gaussian-prior *Miko* backbone—the natural framework into which the LSST/Euclid survey inhomogeneities can be absorbed—and supplies it with the calibrated, co-registered, multi-resolution shear and photo- z catalogs developed here as its data layer. Gradient-based posterior sampling at field-level resolution is made tractable by coupling the pipeline to differentiable *CosmoPower*-like emulators [51, 52], which accelerate the mapping from cosmological parameters to linear and nonlinear power spectra and provide analytic gradients that integrate seamlessly with the *AnaCal* autodiff calibration layer. The same calibrated catalog will further feed downstream analyses targeting the *non-Gaussian* information inaccessible to two-point statistics—log-normal and N -body-prior field-level inference [48–50, 53] and simulation-based or deep-learning analyses using higher-order information [54–56]—broadening the scientific reach of the joint LSST×Euclid catalog beyond any single inference framework.

2 Scientific and Technical Merit

The overarching goal of this project is to deliver, for the first time at survey scale, a joint pixel-level weak-lensing analysis for ground- and space-based imaging from Rubin LSST and Euclid, and to use it to sharpen Rubin LSST’s constraints on dynamical dark energy. The program is organized around four coupled thrusts—a joint LSST×Euclid image-processing pipeline, a Gaussian-prior field-level cosmology analysis, and pathfinder and full-scale analyses on the DES×Euclid-DR1 and LSST-DR1×Euclid-DR2 overlaps, detailed in Section 3. The resulting infrastructure is designed as a foundation for next-generation AI-based image-to-cosmology inference and extends naturally to a joint LSST×Euclid×Roman analysis once Roman data become available.

Scientific Merit

The scientific case for this program rests on four cosmological deliverables, each of which directly addresses one of the outstanding open questions in late-Universe cosmology and feeds into the LSST DESC dark-energy science program.

(1) An independent weak-lensing test of the DESI-motivated hint of dynamical dark energy. The joint analysis improves the LSST weak-lensing constraint on the dynamical dark-energy parameters w_0-w_a by at least $\sim 25\%$ relative to LSST alone, and a Gaussian-prior field-level analysis on the joint footprint adds a complementary, inhomogeneity-aware route to the same signal—together accelerating the survey epoch at which Rubin LSST can deliver an *independent* weak-lensing test of the $3-4\sigma$ hint for time-evolving $w(a)$ from DESI DR2 [7]. Independence is the key: weak lensing probes geometry and late-time growth with degeneracies and systematics distinct from BAO, supernovae, and the CMB, so a consistent result would strengthen the case for dynamical dark energy, while an inconsistent one would point to residual systematics or probe-combination effects.

(2) Sub-percent measurement of S_8 to resolve the S_8 tension. Stage-III cosmic-shear surveys (DES, HSC, KiDS) consistently report values of S_8 that lie $0.5\text{--}2.5\sigma$ below the *Planck* CMB value under Λ CDM (Equation (2)) [57], but lack the statistical reach to discriminate *statistical fluctuation*, *residual systematics*, and *new physics*. Stage-IV surveys provide that reach only if the accompanying systematics budget—shear calibration, cross-redshift blending, photo- z , intrinsic alignments, baryons, and small-scale modeling—is brought under matching sub-percent control. This proposal is built around that requirement: the joint-imaging pipeline of Thrust #1 delivers the sub-percent shear calibration, the raised source density, the improved photometric redshifts, and the selection-bias correction that the budget demands. Together with the LSST-DR1 \times Euclid-DR2 statistical reach, these advances deliver $\sigma(S_8) \lesssim 0.003$, sufficient by construction to classify the S_8 tension.

(3) A validated joint shear catalog for LSST DESC strong-lensing dark-energy and H_0 cosmology. The joint LSST \times Euclid shear catalog produced by this program will anchor the LSST DESC strong-lensing program by tightening the constraint on the *mass-sheet degeneracy* (MSD) [58], which currently limits both time-delay H_0 measurements [59, 60] and tomographic strong-lensing constraints on dark energy [61]. Breaking the MSD requires extending the galaxy–galaxy WL shear profile around strong-lens deflectors down to small angular scales—a projected radius of ~ 0.04 Mpc, corresponding to only a few arcseconds at typical lens redshifts $z \sim 0.5$, just beyond the Einstein radius [62]. The proposed program is well matched to this requirement: joint LSST \times Euclid pixel-level detection and AI-based shape estimation raise the small-scale signal-to-noise on the deflector shear profile. The resulting tightening of the stacked galaxy–galaxy WL constraint on the MSD reaches $\sim 25\%$ relative to LSST-only WL [62], supporting a percent-level H_0 from time-delay cosmography and a tomographic strong-lensing measurement of $w(z)$ to better than 0.1 out to $z \sim 3$, both independent of the CMB and the local distance ladder [61].

(4) A late-time growth anchor for the cosmological neutrino-mass measurement. The proposed joint LSST \times Euclid WL constraint also provides a precise, low-redshift growth anchor for the cosmological sum of neutrino masses $\sum m_\nu$, which suppresses small-scale structure growth in a scale- and redshift-dependent way. Joint analyses of LSST WL + clustering with future CMB-Stage-IV data forecast $\sigma(\sum m_\nu) \sim 30$ meV even in beyond- Λ CDM extensions that vary curvature and the dark-energy equation of state [63], breaking the degeneracies that limit CMB-only constraints and supporting a robust 3σ detection of the minimal ~ 60 meV normal-hierarchy mass once improved CMB optical-depth information is available. The sub-percent-calibrated, joint-imaging shear catalog produced by this program directly enables this neutrino science by ensuring that the neutrino-mass signal in the late-time growth measurement is not absorbed by shear-calibration, photo- z , or survey-inhomogeneity nuisance parameters.

Technical Merit

To deliver the scientific outputs above, the program develops three coupled technical contributions that together form an end-to-end, differentiable, analytically calibrated pipeline running from raw multi-survey pixels to LSST DESC-ready cosmology likelihoods, all at realistic computational and implementation cost.

(1) A joint Rubin \times Euclid pixel-level image-to-catalog pipeline (joint shear and photo- z) with sub-percent bias control and a drop-in interface for AI shear estimators. Building on AnaCal [28, 29, 64], the pipeline replaces image re-rendering in Metadetection with analytical, autodiff-based shear responses propagated consistently across Rubin and Euclid pixel data, controlling $|m| < 0.3\%$ at survey scale at $\sim 100\times$ lower calibration cost than Metadetection—a speedup that brings survey-scale joint-imaging catalogs within standard LSST DESC compute and, through the same differentiable construction (coupled to CosmoPower emulators), supplies the analytic gradients that make downstream gradient-based field-level cosmology inference tractable. Joint pixel-level detection across the deep multi-band Rubin and the high-

resolution stable-PSF Euclid imaging raises the LSST WL n_{eff} by at least $\sim 50\%$ at the catalog level [10], with image-level processing expected to deliver more [11]. Pixel-level forced photometry on the same LSST *ugrizy* + Euclid NIR images delivers consistent *u*-through-*H* fluxes for every detected source, avoiding catalog-matching ambiguities; ingested into the LSST DESC RAIL [36, 37] estimators, the joint photometry cuts the catastrophic-outlier rate by 30–40% at $z \gtrsim 1$ [14, 15] and de-biases the tomographic $n(z)$. The same differentiable framework propagates analytical *magnitude* responses to shear through the tomographic binning step, correcting the selection-induced multiplicative bias that leaks into $n(z)$ —to our knowledge the first end-to-end propagation of the magnitude–shear response in a Stage-IV WL pipeline. The modular, differentiable structure also serves as a drop-in backbone for AI shear estimators: the D_4 -equivariant-CNN [12] and denoising-score-matching extensions [13] inherit AnaCal’s analytical calibration through automatic differentiation and cut shape noise by another 10–20%, and the same interface extends to **DeepDISC** [65–67] and to foundation models such as **AION-1** [68]. The combined gain in effective source density from joint detection and AI-based shape estimation, together with the sharper joint photometric redshifts, propagates through the Fisher-forecast scaling relation between the dark-energy figure of merit and the effective source density [69] into an improvement of at least 25% in the LSST weak-lensing constraint on w_0 and w_a .

(2) End-to-end validation and reusable LSST DESC data products. $|m| < 0.3\%$ validation at survey scale requires controlled simulations of blending, anisotropic and chromatic PSFs [39–41], and detection systematics. The pipeline will be exercised on a continuous-integration basis against the PI-codeveloped *descwl-shear-sims* (the established LSST DESC shear-bias-validation tool) wired into the LSST *imSim* [70–72] framework, sharing identical inputs with Rubin Operations and DESC validation runs. The validated outputs—coadded multi-survey image stacks of the Rubin Deep Drilling Fields (DDFs) and overlapping Euclid/Roman deep fields, plus object catalogs, photo-*z* training sets, and shear responses—are packaged as a reusable LSST DESC data product leveraged by the cosmic-shear, cluster, photo-*z*, and strong-lensing working groups.

(3) A differentiable, emulator-accelerated field-level inference backbone. The calibrated, co-registered shear and photo-*z* catalog feeds the Gaussian-prior Miko [46] engine, with each LSST-only / Euclid-only / overlap region entering the forward model with its own number density, shape noise, and $n(z)$ so that survey inhomogeneity is absorbed by construction. Gradient-based posterior sampling at field-level resolution is made tractable by coupling Miko to the differentiable CosmoPower [51, 52] emulators, which provide analytic gradients of the linear and nonlinear power spectra and integrate seamlessly with the AnaCal autodiff calibration layer—yielding an end-to-end-differentiable stack from raw pixels to the cosmological posterior.

The proposed work will be carried out within the LSST DESC, primarily in the *Pixel-to-Object* and *Photometric Redshift* working groups, with the resulting joint catalogs and simulations delivered to the large-scale-structure, cluster, and strong-lensing working groups for downstream cosmological analysis.

3 Proposed Research and Methods

The proposed methodology is organized into four coupled thrusts that together deliver an end-to-end, differentiable joint LSST×Euclid weak-lensing analysis: (#1) the joint image-processing pipeline (joint detection, joint shape measurement with chromatic-PSF correction, and joint flux and photo-*z*); (#2) Gaussian-prior field-level cosmology analysis on the resulting calibrated catalog; (#3) the DES×Euclid-DR1 pathfinder analysis; and (#4) the LSST-DR1×Euclid-DR2 analysis. For each thrust we describe the method and why it is appropriate and timely for the LSST-DR1 / Euclid-DR2 schedule.

Thrust #1: Joint LSST×Euclid image processing pipeline

Method. The joint pipeline ingests overlapping LSST and Euclid imaging and delivers a co-registered shear and photometric-redshift catalog through three chained AnaCal modules in which the analytical pixel-level shear response is propagated by automatic differentiation end-to-end: (i) *joint detection* on a combined log-likelihood map built from Euclid VIS and LSST imaging oversampled onto the Euclid pixel grid, so the analytical detection-bias correction [28] propagates through the joint map by construction; (ii) *joint shape measurement* on the joint pixel data using three complementary AnaCal-calibrated estimators—Fourier moments [64], galaxy model fitting [35], and physics-informed D_4 -equivariant CNN feature extractors [12] optionally augmented with denoising score matching [13]—with chromatic-PSF corrections [40, 41] for the Euclid VIS and NISP bands constrained by overlapping LSST *ugrizy* and Roman NIR imaging; (iii) *joint flux and photometric-redshift estimation* in all LSST *ugrizy* and Euclid VIS + NISP bands using fixed-aperture photometry feeding the LSST DESC RAIL/FlexZBoost [36, 37] estimator, with the analytical shear response propagated through to the photometric redshift itself.

Appropriate. AnaCal delivers sub-percent multiplicative-bias control on the moment-based, model-fitting, and AI feature families [12, 29, 35], while joint LSST–Euclid pixel-level detection and shape measurement raises the effective galaxy number density and reduces the shape noise on the LSST WL sample relative to LSST-only processing [10, 11]. Adding Euclid NIR photometry to LSST *ugrizy* further reduces the catastrophic photo- z outlier rate by 30–40% at $z \gtrsim 1$ [14, 15], and propagating the shear response analytically all the way to the photo- z estimate corrects the magnitude-cut selection bias in closed form—a step that has not previously been implemented end-to-end in any Stage-IV WL pipeline. Validation is performed in `descwl-shear-sims/imSim` [70–72] with controlled truth shear distortions.

Timely. The AnaCal + RAIL backbone is already deployed at survey scale on HSC-Y6 and LSST DP1, and is currently being applied to LSST DP2 [29, 38]—providing a validated single-survey baseline on which the joint extension is a small delta. The physics-informed AI shear estimators [12, 13] and the chromatic-PSF correction methodology [40, 41] have both been developed in the past two years and are ready to be ingested into the joint-imaging pipeline. The required LSST+Euclid overlap becomes available with Euclid-DR1 and the DES–Euclid-DR1 pathfinder fields at the start of FY27, and the Roman overlap needed for LSST-Y1-precision chromatic-PSF correction follows in the FY29–FY30 window, exactly aligned with Thrusts #3 and #4.

Thrust #2: Field-level cosmology analysis pipeline

Method. The calibrated, co-registered shear and photo- z catalog from Thrust #1 is fed into the Gaussian-prior Miko [46] field-level inference engine. The forward model partitions the survey footprint into LSST-only, Euclid-only, and LSST–Euclid overlap subregions, and assigns each subregion its own depth, shape-noise level, source number density, PSF, blending, and photo- z model, so that survey inhomogeneity is absorbed into the likelihood by construction. Posterior sampling over cosmological and nuisance parameters at field-level resolution is made tractable by coupling Miko to the differentiable cosmological emulators CosmoPower [51] and CosmoPower-JAX [52], which provide analytical gradients of the linear and nonlinear matter power spectra with respect to the cosmological parameters. These gradients integrate seamlessly with the AnaCal autodiff calibration layer of Thrust #1, yielding an end-to-end-differentiable stack from raw pixels to the cosmological posterior.

Appropriate. A Gaussian-prior field-level analysis has been demonstrated to recover *unbiased* tomographic power-spectrum amplitudes on HSC Year-3-like mocks [46], in contrast to log-normal field-level priors that introduce significant prior misspecification bias [48, 49]. The forward-model treatment of survey inhomogeneity is the natural way to combine LSST-only, Euclid-only, and LSST–Euclid overlap regions coherently,

avoiding the residual inhomogeneity systematics that limit catalog-level cosmic-shear analyses at Stage-IV precision [45].

Timely. The Miko pipeline and the CosmoPower-JAX emulators are publicly released and already validated, so the field-level analysis can be deployed immediately on the joint LSST-DR1 / Euclid-DR2 catalog produced by Thrust #1 in the FY29–FY30 window. Downstream, the same calibrated catalog will also feed log-normal and N -body-prior field-level inference [48–50, 53] and simulation-based / deep-learning cosmology analyses based on higher-order summaries [54–56], broadening the scientific reach beyond the Gaussian-prior baseline.

Thrust #3: DES×Euclid-DR1 pathfinder analysis

Method. We apply the Thrust #1 joint pipeline to the $\sim 1,000 \text{ deg}^2$ DES×Euclid-DR1 overlap to produce a joint shear and photo- z catalog; carry out null tests of PSF modeling, shear estimation, and star–galaxy correlations using the LSST DESC TXPipe [73] framework; and feed the catalog into the Thrust #2 field-level cosmology pipeline. The DES Y6 shear catalog is used over the non-overlapping DES footprint to extend the cosmic-shear constraint beyond the DES×Euclid-DR1 overlap.

Appropriate. The DES×Euclid-DR1 overlap is the first ground×space WL dataset at a depth comparable to LSST-Y1, and is therefore the natural proving ground for the joint image-processing pipeline before it is brought into production on the LSST-DR1×Euclid overlap. TXPipe is the mature LSST DESC null-test infrastructure, and the DES Y6 shear catalog provides a benchmark against which the joint-imaging cosmic-shear constraint can be cross-validated.

Timely. Euclid-DR1 is released at the start of FY27, exactly aligned with the start of this proposal; TXPipe is publicly available; and the DES Y6 shear catalog will be released during the pathfinder window.

Thrust #4: LSST-DR1×Euclid-DR2 analysis

Method. Building on the Thrust #3 pathfinder result, we run the Thrust #1 joint pipeline on the $> 3,000 \text{ deg}^2$ LSST-DR1×Euclid-DR2 overlap to deliver a calibrated joint shear and photo- z catalog, perform TXPipe null tests, and feed the catalog into the Thrust #2 field-level cosmology pipeline to deliver the first joint-imaging WL constraint on w_0-w_a . The shear catalog is validated against the LSST DESC SRD shear-bias requirement using an LSST-Y1-scale `descwl-shear-sims/imSim` [70–72] simulation campaign.

Appropriate. LSST-DR1×Euclid-DR2 is the first joint ground×space WL dataset that reaches LSST-Y1 depth and the LSST DESC SRD systematic-error requirements, making it the dataset on which the joint pipeline produces its primary cosmological deliverable.

Timely. LSST-DR1 is released in June 2028 and Euclid-DR2 in March 2029, so the $> 3,000 \text{ deg}^2$ overlap becomes available in the middle of FY29. By that time the joint pipeline has been validated end-to-end on the Thrust #3 DES×Euclid-DR1 pathfinder, allowing immediate deployment.

4 Timetable of Activities

The proposed program is organized into a five-year plan that is tightly synchronized with the Stage-IV imaging-survey data-release schedule: Euclid-DR1 (21 October 2026), Roman launch (by May 2027), LSST-DR1 (June 2028), Euclid-DR2 (March 2029), and LSST-DR2 (anticipated 2030). Each year couples a methodology deliverable to a real-data deliverable, with built-in risk-buffer fallbacks that keep the program productive if any single survey schedule slips, as illustrated in Figure 6. **Each year requires 50%**

full-time equivalent (FTE) of the PI and 100% FTE of one postdoctoral researcher (PD).

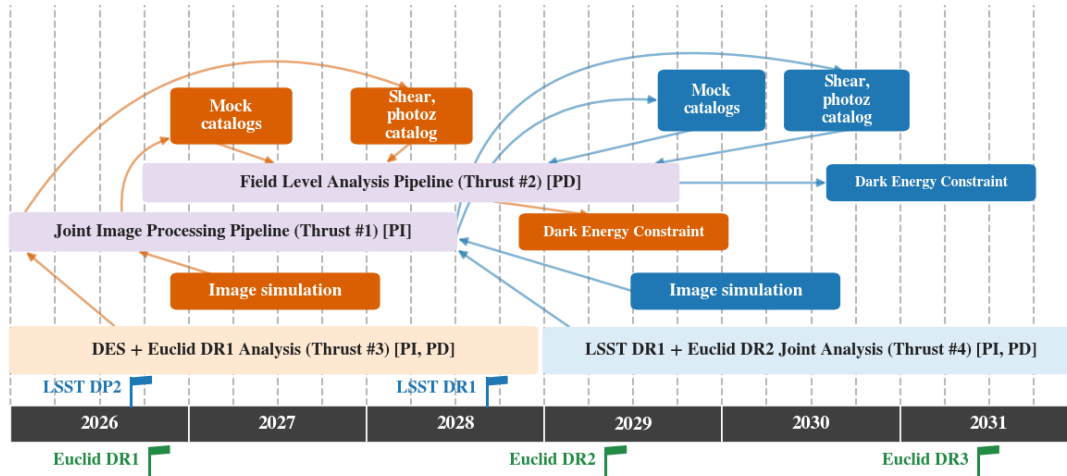


Figure 6: Five-year timeline of the proposed program, aligned with the Stage-IV imaging-survey data-release schedule (LSST-DP2, Euclid-DR1, LSST-DR1, Euclid-DR2, Euclid-DR3). Transparent boxes mark the four program thrusts—purple for the methodology backbones (Thrust #1 joint image-processing pipeline, Thrust #2 field-level analysis pipeline), orange for Thrust #3 (DES×Euclid-DR1 pathfinder), and blue for Thrust #4 (LSST-DR1×Euclid-DR2 joint analysis)—with their horizontal extent indicating the active period on the timeline. Solid orange and blue boxes are the per-thrust deliverables (image simulations, mock catalogs, shear+photo- z catalogs, and dark-energy constraints), positioned at the time they are produced. Arrows show data and product flow between deliverables and pipelines.

The first two and a half years build and validate the joint image-processing pipeline (Thrust #1) and the field-level cosmology backbone (Thrust #2) through the DES×Euclid-DR1 pathfinder analysis (Thrust #3) on the $\sim 1,000 \text{ deg}^2$ DES×Euclid-DR1 overlap, which is comparable in depth to LSST-Y1. The remaining two and a half years carry the validated pipeline into production on the $> 3,000 \text{ deg}^2$ LSST-DR1×Euclid-DR2 overlap (Thrust #4), fully coordinated with the LSST DESC DR1 analysis. The LSST-DP2 footprint does not provide sufficient overlap with Euclid to support a joint shear analysis, so no intermediate LSST-DP2 deployment is attempted.

Year 1 (FY26–FY27): Build the joint image-processing pipeline (Thrust #1). Extend AnaCal [29] from single-survey to multi-resolution, multi-survey joint imaging: joint detection with analytical detection-bias propagation; moment-based, model-fitting, and physics-informed D_4 -equivariant CNN shape estimators; and joint flux + RAIL photo- z with the analytical shear response carried through to the photometric redshift. Build the overlapped ground-space image-simulation suite within descwl-shear-sims/imSim [70–72], with controlled truth shear, realistic PSFs and pixel scales, and survey-specific noise. **Deliverables:** a public release of the joint-imaging AnaCal pipeline; the overlapped ground-space image-simulation suite; and a journal paper documenting the pipeline and its simulation tests.

Year 2 (FY27–FY28): From images to pathfinder catalogs (Thrusts #1/#3). Apply the pipeline to the DES×Euclid-DR1 overlap. Carry out TXPipe [73] null tests of PSF modeling, shear estimation, and star-galaxy shape correlations, and compare WL cluster mass estimates against the DES Y6 baseline. Calibrate the joint photometric redshifts against the rich spectroscopic sample in the Extended Chandra Deep Field–South (ECDFS), processed end-to-end in the LSST DESC RAIL [37] framework, to anchor the joint $n(z)$

tomography with a spectroscopic-quality redshift truth set. **Deliverables:** a public DES×Euclid-DR1 joint shear catalog with joint photo- z estimates covering the overlapping $\sim 1,000 \text{ deg}^2$; one journal paper presenting the shear catalog and its null tests, and a companion paper presenting the photo- z catalog with its standard validation.

Year 3 (FY28–FY29): Pathfinder cosmology and chromatic-PSF deployment (Thrusts #1/#2/#3). Complete the DES×Euclid-DR1 pathfinder program with a Gaussian-prior field-level cosmology analysis on the joint shear and photo- z catalogs above, using the Miko [46] engine coupled to the differentiable CosmoPower [51, 52] emulators, with a self-consistent forward-model treatment of shear bias, intrinsic alignments, photo- z uncertainty, and survey inhomogeneity, and extend the cosmic-shear constraint beyond the overlap using the DES Y6 shear catalog. The result will be benchmarked against the DES Y6 cosmic-shear baseline. In parallel, deploy the chromatic-PSF correction component of Thrust #1 at LSST-Y1 systematics precision using the LSST-DR1 + Roman overlap that becomes available in this window [40, 41]. **Deliverables:** cosmological parameter posteriors from the DES×Euclid-DR1 joint analysis; a journal paper reporting the cosmic-shear cosmology analysis; and updated chromatic-PSF models for the Euclid VIS and NISP bands with their PSF-systematics tests.

Year 4 (FY29–FY30): From images to the LSST-DR1×Euclid-DR2 catalog (Thrusts #1/#4). Run the full joint pipeline on the $> 3,000 \text{ deg}^2$ LSST-DR1×Euclid-DR2 overlap as Euclid-DR2 becomes available (March 2029), perform TXPipe null tests and cross-survey validation, and quantify residual shear and selection biases. In parallel, build the image-simulation suite at LSST-Y1 scale on top of imSim and use it to calibrate the joint shear catalog against the LSST DESC SRD shear-bias requirement. **Deliverables:** a public LSST-Y1 joint image-simulation suite; a calibrated LSST-DR1×Euclid-DR2 joint shear catalog; one journal paper documenting the image-simulation tests and shear-bias calibration; and a companion paper presenting the joint shear catalog and its null-test validation.

Year 5 (FY30–FY31): Joint LSST×Euclid field-level dark-energy analysis (Thrusts #2/#4). Use the validated joint catalog to perform a Gaussian-prior field-level cosmology analysis on the LSST-DR1×Euclid-DR2 overlap with Miko [46] coupled to CosmoPower [51, 52], delivering the first joint-imaging WL constraint on w_0-w_a . Combine with DESI BAO and *Planck* CMB priors to deliver an independent Stage-IV cross-check of the DESI dynamical-dark-energy hint, and establish the joint-pipeline foundation for the LSST-DR2 era by delivering tools and catalogs to the LSST DESC large-scale-structure (LSS) and cluster working groups for downstream WL science. **Deliverables:** cosmological parameter posteriors from the joint-imaging WL field-level analysis; a peer-reviewed publication of the dark-energy result; and a DESC-supported public release of the joint LSST×Euclid analysis pipeline and simulation infrastructure.

Contingencies and Risk Mitigation

Image-processing complexity. The joint image-processing pipeline extends AnaCal [29], a shear-calibration framework already derived, implemented, and validated at survey scale by the PI on HSC and on the LSST Commissioning Camera DP1, so the proposed work adapts a mature single-survey framework to multi-resolution, multi-survey joint imaging rather than building a new pipeline from scratch. It also builds directly on LSST DESC’s substantial investment in image reduction: the PI is one of the LSST DESC pipeline scientists supporting that effort, and develops the joint shear estimation as a direct extension of it. The AI components of the joint shear measurement follow a start-simple, integrate-first strategy—beginning from a simple CNN baseline and adding complexity (physics-informed D_4 -equivariant architectures, denoising score matching) incrementally, only where it demonstrably improves performance—and are further de-risked by the Laboratory Directed Research and Development (LDRD) program at Brookhaven National Laboratory, which supports preparatory work on AI-based shear estimation before this program begins.

Together these foundations substantially lower the technical risk of Thrust #1.

Euclid data availability. The schedule depends on the Euclid-DR1 (October 2026) and Euclid-DR2 (March 2029) releases. If Euclid-DR1 slips, the Thrust #3 pathfinder proceeds on the Euclid Quick Release (Q2) data over the same fields; if Euclid-DR2 slips, Thrust #4 begins on the Euclid-DR1 footprint. In both cases an earlier Euclid release is already in hand before the nominal date, so the program stays productive without waiting on the full release.

Euclid data products. If Euclid releases only single-visit exposures and withholds the cosmology-grade coadds, the joint pipeline falls back to running source detection on the deeper DES (Thrust #3) or LSST (Thrust #4) coadds and performing forced joint shear measurement on the Euclid single-visit exposures together with the LSST images at the detected positions. Because AnaCal’s analytical shear response is derived at the pixel level, it applies natively to forced measurement on single-visit Euclid frames, so this fallback preserves the joint ground-space WL science with only a modest reduction in high-resolution depth.

Field-level pipeline complexity. Thrust #2’s Gaussian-prior field-level inference is the most methodologically novel element of the program; it drives the cosmological analyses of Thrust #3 (the DES×Euclid-DR1 pathfinder, Year 3) and Thrust #4 (the LSST-DR1×Euclid-DR2 analysis, Year 5). Should its validation on mock catalogs from the joint image-processing pipeline not complete on schedule, each analysis falls back to a standard two-point cosmic-shear analysis of the calibrated joint catalog: the joint LSST×Euclid two-point signal in Thrust #4, for example, is then measured separately on the LSST-only and LSST×Euclid-overlap regions—each with its own redshift distribution and shape noise—and Thrust #3 likewise on its DES-only and DES×Euclid-overlap regions. This fallback neglects the cross-correlation between regions and does not reach the optimal joint-survey constraint, but still delivers the central dark-energy result on a mature, well-validated analysis path while the field-level pipeline is completed.

5 Competency of Applicant’s Personnel and Adequacy of Proposed Resources

PI track record. The PI developed the AnaCal analytical shear-calibration framework from first principles—deriving the analytical pixel-level shear response, the analytical detection-bias correction [28], and the analytical noise-bias correction [29] that together constitute the AnaCal formalism—and wrote the entire AnaCal code base from scratch [35]. Building on this foundation, the PI has consistently delivered survey-scale weak-lensing shear catalogs and cosmic-shear analyses for the most demanding cosmology surveys of the past decade: led the HSC Y3 image-simulation campaign and shear catalog production [74] and the subsequent HSC Y3 cosmic-shear cosmology analyses [75–77], developed the HSC Y6 image-simulation suite for shear calibration, is leading the ongoing HSC Y6 shear catalog, produced the LSST Commissioning Camera DP1 AnaCal shear catalog [38], and is currently leading the LSST DP2 AnaCal shear catalog. The PI is also supervising graduate students applying AnaCal to calibrate AI-based shear estimators [12, 13], and has co-supervised the graduate student who developed the Miko field-level weak-lensing inference pipeline [46]—giving the PI direct training-the-trainer experience that maps onto both the AI-extension and field-level-inference thrusts of this proposal.

Role within LSST DESC. The PI is a pipeline scientist within LSST DESC, the collaboration responsible for LSST’s dark-energy cosmology analyses—a coordinating role in which the PI aligns the AnaCal shear-measurement and image-processing effort with the collaboration’s pixel-processing, photometric-redshift, and cosmology working groups. Because the joint LSST×Euclid pipeline proposed here will be developed and delivered inside DESC, its catalogs, simulations, and software feed directly into the collaboration’s dark-energy analysis path. This standing gives the PI the coordination channels and institutional buy-in to carry the joint pipeline from method development through to a collaboration-adopted analysis, ensuring the proposed work strengthens the LSST cosmology program rather than developing in isolation.

Host institution. The PI is employed at Brookhaven National Laboratory (BNL), which regularly attracts top-tier postdoctoral scholars to its Cosmology and Astrophysics group. BNL has a long tradition of leadership in weak-lensing shear measurement, catalog production, and cosmological analysis, dating back to the founding contributions of Erin Sheldon to the Sloan Digital Sky Survey (SDSS), DES, and LSST WL programs and continued through the PI's work on the HSC and LSST WL pipelines—providing exactly the institutional expertise required to deliver the joint Rubin×Euclid pipeline proposed here.

Scientific Computing and Data Facilities. The proposal also relies on world-class computational facilities through BNL's Scientific Data and Computing Center (SDCC), a DOE-recognized high-performance computing (HPC) and large-scale data-handling center supporting the LSST, ATLAS, DUNE, and DESI experiments, among others. SDCC provides petabyte-scale storage, GPU-equipped HPC nodes, and a direct, low-latency connection to NERSC and to the LSST/Rubin Data Management infrastructure. These resources are essential for the overlapped ground-space image simulations, joint-survey image processing, and end-to-end shear-pipeline validation that underpin the proposed work, and are already in routine use by the PI's group for LSST DP1/DP2 AnaCal shear analyses.

6 Potential For Leadership Within the Scientific Community

Through the development of the AnaCal analytical shear-calibration framework and its deployment across the leading imaging surveys of the past decade—and as convener of the HSC weak-lensing working group—the PI has established a recognized position in weak-lensing shear measurement. This program is the platform from which that position grows into scientific leadership of the joint-imaging, AI-driven era of weak-lensing cosmology now beginning.

The defining opportunity of the coming decade is the infusion of artificial intelligence into cosmological data analysis, and this program positions the PI to lead it for weak lensing along two fronts. The first is *speed*: AnaCal's analytical, autodiff-based construction already cuts shear-catalog production cost by $\sim 100\times$, and coupling it to differentiable emulators makes gradient-based field-level inference—previously intractable at survey scale—routine, turning a multi-survey image-to-cosmology analysis into a fast, end-to-end-differentiable computation. The second is *constraining power*: physics-informed AI shear estimators, and ultimately astronomical foundation models, extract more cosmological signal per galaxy than hand-crafted methods while preserving the sub-percent calibration that dark-energy cosmology demands. By making AI simultaneously fast and calibratable for weak lensing, the PI will help set the methodological direction by which the field turns Stage-IV imaging into dark-energy and cosmological constraints—an effort directly aligned with the DOE Genesis Mission to accelerate scientific discovery with AI.

This leadership extends beyond methodology. The joint pipeline makes the PI a natural bridge between the U.S. DOE/NSF Rubin LSST program and the ESA Euclid and NASA Roman missions, and the open-source release of AnaCal with its joint-imaging and field-level extensions will establish these tools as a shared community standard. By training graduate students and postdoctoral researchers at the intersection of weak lensing, artificial intelligence, and cosmological inference, the PI will build a research group—and a strengthened role for Brookhaven National Laboratory within LSST DESC—equipped to carry joint, AI-driven weak-lensing cosmology through the LSST decade and into the Roman era.

APPENDIX 1: Bibliography & References

- [1] Michel Chevallier and David Polarski. “Accelerating Universes with Scaling Dark Matter”. In: *International Journal of Modern Physics D* 10.2 (Jan. 2001), pp. 213–223. arXiv: [gr-qc/0009008 \[gr-qc\]](#).
- [2] Ž. Ivezić, S. M. Kahn, J. A. Tyson, et al. “LSST: From Science Drivers to Reference Design and Anticipated Data Products”. In: *ApJ* 873.2, 111 (Mar. 2019), p. 111. arXiv: [0805.2366 \[astro-ph\]](#).
- [3] DESI Collaboration. “The DESI Experiment Part I: Science, Targeting, and Survey Design”. In: *arXiv e-prints*, arXiv:1611.00036 (Oct. 2016), arXiv:1611.00036. arXiv: [1611.00036 \[astro-ph.IM\]](#).
- [4] Daniel J. Eisenstein, Idit Zehavi, David W. Hogg, et al. “Detection of the Baryon Acoustic Peak in the Large-Scale Correlation Function of SDSS Luminous Red Galaxies”. In: *ApJ* 633.2 (Nov. 2005), pp. 560–574. arXiv: [astro-ph/0501171 \[astro-ph\]](#).
- [5] A. G. Adame et al. “DESI 2024 VI: cosmological constraints from the measurements of baryon acoustic oscillations”. In: *JCAP* 2025.2, 021 (Feb. 2025), p. 021. arXiv: [2404.03002 \[astro-ph.CO\]](#).
- [6] DESI Collaboration, M. Abdul-Karim, et al. “DESI DR2 results. II. Measurements of baryon acoustic oscillations and cosmological constraints”. In: *Phys. Rev. D* 112.8, 083515 (Oct. 2025), p. 083515. arXiv: [2503.14738 \[astro-ph.CO\]](#).
- [7] DESI Collaboration, K. Lodha, et al. “Extended dark energy analysis using DESI DR2 BAO measurements”. In: *Phys. Rev. D* 112.8, 083511 (Oct. 2025), p. 083511. arXiv: [2503.14743 \[astro-ph.CO\]](#).
- [8] Judit Prat and David Bacon. “Weak gravitational lensing”. In: *Encyclopedia of Astrophysics*. Vol. 5. Elsevier, Jan. 2026, pp. 508–537. arXiv: [2501.07938 \[astro-ph.CO\]](#).
- [9] Euclid Collaboration. “Euclid: I. Overview of the Euclid mission”. In: *A&A* 697, A1 (May 2025), A1. arXiv: [2405.13491 \[astro-ph.CO\]](#).
- [10] R. L. Schuhmann, C. Heymans, and J. Zuntz. “Galaxy shape measurement synergies between LSST and Euclid”. In: *arXiv e-prints*, arXiv:1901.08586 (Jan. 2019), arXiv:1901.08586. arXiv: [1901.08586 \[astro-ph.IM\]](#).
- [11] R. Chary et al. “Joint Survey Processing of Euclid, Rubin and Roman: Final Report”. In: *arXiv e-prints*, arXiv:2008.10663 (Aug. 2020), arXiv:2008.10663. arXiv: [2008.10663 \[astro-ph.IM\]](#).
- [12] Shurui Lin, Xiangchong Li, Ji Li, Shengcao Cao, Xin Liu, et al. “D₄CNN×AnaCal: Physics-Informed Machine Learning for Accurate and Precise Weak Lensing Shear Estimation”. In: *arXiv e-prints* (Mar. 2026). arXiv: [2603.19046 \[astro-ph.IM\]](#).
- [13] Shurui Lin, Xiangchong Li, Xin Liu, et al. “D₄CNN×AnaCal II: Shear Response as a Score Inner Product: A Unified Statistical Framework for Weak Gravitational Lensing Shear Estimation”. In: *in preparation* (2026).
- [14] Melissa L. Graham, Andrew J. Connolly, Željko Ivezić, Samuel J. Schmidt, R. Lynne Jones, et al. “Photometric Redshifts with the LSST. II. The Impact of Near-infrared and Near-ultraviolet Photometry”. In: *AJ* 159.6, 258 (June 2020), p. 258. arXiv: [2004.07885 \[astro-ph.IM\]](#).
- [15] B. Jain, D. Spergel, R. Bean, A. Connolly, et al. “The Whole is Greater than the Sum of the Parts: Optimizing the Joint Science Return from LSST, Euclid and WFIRST”. In: *arXiv e-prints*, arXiv:1501.07897 (Jan. 2015), arXiv:1501.07897. arXiv: [1501.07897 \[astro-ph.IM\]](#).
- [16] D. Spergel et al. “Wide-Field Infrared Survey Telescope-Astrophysics Focused Telescope Assets WFIRST-AFTA 2015 Report”. In: *arXiv e-prints*, arXiv:1503.03757 (Mar. 2015), arXiv:1503.03757. arXiv: [1503.03757 \[astro-ph.IM\]](#).

-
- [17] Matthias Bartelmann and Peter Schneider. “Weak gravitational lensing”. In: *Phys. Rep.* 340.4-5 (Jan. 2001), pp. 291–472. arXiv: [astro-ph/9912508](#) [[astro-ph](#)].
- [18] Henk Hoekstra and Bhuvnesh Jain. “Weak Gravitational Lensing and Its Cosmological Applications”. In: *Annual Review of Nuclear and Particle Science* 58.1 (Nov. 2008), pp. 99–123. arXiv: [0805.0139](#) [[astro-ph](#)].
- [19] Martin Kilbinger. “Cosmology with cosmic shear observations: a review”. In: *Reports on Progress in Physics* 78.8, 086901 (July 2015), p. 086901. arXiv: [1411.0115](#) [[astro-ph.CO](#)].
- [20] Rachel Mandelbaum. “Weak Lensing for Precision Cosmology”. In: *ARA&A* 56 (Sept. 2018), pp. 393–433. arXiv: [1710.03235](#) [[astro-ph.CO](#)].
- [21] The Dark Energy Survey Collaboration. “The Dark Energy Survey: more than dark energy - an overview”. In: *MNRAS* 460.2 (Aug. 2016), pp. 1270–1299. arXiv: [1601.00329](#) [[astro-ph.CO](#)].
- [22] H. Aihara, N. Arimoto, R. Armstrong, et al. “The Hyper Suprime-Cam SSP Survey: Overview and survey design”. In: *PASJ* 70, S4 (Jan. 2018), S4. arXiv: [1704.05858](#) [[astro-ph.IM](#)].
- [23] J. T. A. de Jong, G. A. Verdoes Kleijn, K. H. Kuijken, and E. A. Valentijn. “The Kilo-Degree Survey”. In: *Experimental Astronomy* 35.1-2 (Jan. 2013), pp. 25–44. arXiv: [1206.1254](#) [[astro-ph.CO](#)].
- [24] Planck Collaboration, N. Aghanim, Y. Akrami, et al. “Planck 2018 results. VI. Cosmological parameters”. In: *A&A* 641, A6 (Sept. 2020), A6. arXiv: [1807.06209](#) [[astro-ph.CO](#)].
- [25] The LSST Dark Energy Science Collaboration, R. Mandelbaum, T. Eifler, et al. “The LSST Dark Energy Science Collaboration (DESC) Science Requirements Document”. In: *arXiv e-prints*, arXiv:1809.01669 (Sept. 2018), arXiv:1809.01669. arXiv: [1809.01669](#) [[astro-ph.CO](#)].
- [26] P. Capak et al. “Enhancing LSST Science with Euclid Synergy”. In: *arXiv e-prints*, arXiv:1904.10439 (Apr. 2019), arXiv:1904.10439. arXiv: [1904.10439](#) [[astro-ph.IM](#)].
- [27] A. Merloni, G. Lamer, T. Liu, M. E. Ramos-Ceja, et al. “The SRG/eROSITA all-sky survey. First X-ray catalogues and data release of the western Galactic hemisphere”. In: *A&A* 682, A34 (Feb. 2024), A34. arXiv: [2401.17274](#) [[astro-ph.HE](#)].
- [28] Xiangchong Li and Rachel Mandelbaum. “Analytical weak-lensing shear responses of galaxy properties and galaxy detection”. In: *MNRAS* 521.4 (June 2023), pp. 4904–4926. arXiv: [2208.10522](#) [[astro-ph.CO](#)].
- [29] Xiangchong Li, Rachel Mandelbaum, and The LSST Dark Energy Science Collaboration. “Analytical noise bias correction for precise weak lensing shear inference”. In: *MNRAS* 536.4 (Feb. 2025), pp. 3663–3676. arXiv: [2408.06337](#) [[astro-ph.CO](#)].
- [30] Richard Massey, Catherine Heymans, Joel Bergé, Gary Bernstein, Sarah Bridle, et al. “The Shear Testing Programme 2: Factors affecting high-precision weak-lensing analyses”. In: *MNRAS* 376.1 (Mar. 2007), pp. 13–38. arXiv: [astro-ph/0608643](#) [[astro-ph](#)].
- [31] Dragan Huterer, Masahiro Takada, Gary Bernstein, and Bhuvnesh Jain. “Systematic errors in future weak-lensing surveys: requirements and prospects for self-calibration”. In: *MNRAS* 366.1 (Feb. 2006), pp. 101–114. arXiv: [astro-ph/0506030](#) [[astro-ph](#)].
- [32] Eric Huff and Rachel Mandelbaum. “Metacalibration: Direct Self-Calibration of Biases in Shear Measurement”. In: *arXiv e-prints*, arXiv:1702.02600 (Feb. 2017), arXiv:1702.02600. arXiv: [1702.02600](#) [[astro-ph.CO](#)].
- [33] E. S. Sheldon and E. M. Huff. “Practical Weak-lensing Shear Measurement with Metacalibration”. In: *ApJ* 841.1, 24 (May 2017), p. 24. arXiv: [1702.02601](#) [[astro-ph.CO](#)].
-

-
- [34] E. S. Sheldon, M. R. Becker, N. MacCrann, and M. Jarvis. “Mitigating Shear-dependent Object Detection Biases with Metacalibration”. In: *ApJ* 902.2, 138 (Oct. 2020), p. 138. arXiv: 1911.02505 [astro-ph.CO].
- [35] Xiangchong Li. “Analytical weak-lensing shear response of galaxy model fitting”. In: *arXiv e-prints*, arXiv:2506.16607 (June 2025), arXiv:2506.16607. arXiv: 2506.16607 [astro-ph.CO].
- [36] Rafael Izbicki and Ann B. Lee. “Converting high-dimensional regression to high-dimensional conditional density estimation”. In: *Electronic Journal of Statistics* 11.2 (2017), pp. 2800–2831.
- [37] The RAIL Team et al. “Redshift Assessment Infrastructure Layers (RAIL): Rubin-era photometric redshift stress-testing and at-scale production”. In: *The Open Journal of Astrophysics* 9 (Feb. 2026), p. 58200. arXiv: 2505.02928 [astro-ph.IM].
- [38] Xiangchong Li et al. *AnaCal Shear Profile of Abell 360 in LSST ComCam Data Preview 1*. SIT-COMTN 164. LSST Project / Vera C. Rubin Observatory, 2025.
- [39] Joshua E. Meyers and Patricia R. Burchat. “Impact of Atmospheric Chromatic Effects on Weak Lensing Measurements”. In: *ApJ* 807.2, 182 (July 2015), p. 182. arXiv: 1409.6273 [astro-ph.CO].
- [40] Federico Berlfein, Rachel Mandelbaum, Xiangchong Li, et al. “Chromatic effects on the PSF and shear measurement for the Roman Space Telescope High-Latitude Wide Area Survey”. In: *MNRAS* 542.2 (Sept. 2025), pp. 608–628. arXiv: 2505.00093 [astro-ph.CO].
- [41] Federico Berlfein, Rachel Mandelbaum, Jiachuan Xu, and Tianqing Zhang. “Optimizing the Roman Space Telescope High-Latitude Wide Area Survey for mitigating chromatic PSF effects on shear measurement”. In: *arXiv e-prints*, arXiv:2603.15763 (Mar. 2026), arXiv:2603.15763. arXiv: 2603.15763 [astro-ph.CO].
- [42] M. Tewes, T. Kuntzer, R. Nakajima, F. Courbin, H. Hildebrandt, et al. “Weak-lensing shear measurement with machine learning. Teaching artificial neural networks about feature noise”. In: *A&A* 621, A36 (Jan. 2019), A36. arXiv: 1807.02120 [astro-ph.CO].
- [43] Zekang Zhang, Huanyuan Shan, Nan Li, et al. “FORKLENS: Accurate weak-lensing shear measurement with deep learning”. In: *A&A* 683, A209 (Mar. 2024), A209. arXiv: 2301.02986 [astro-ph.CO].
- [44] Taco S. Cohen and Max Welling. “Group Equivariant Convolutional Networks”. In: *arXiv e-prints*, arXiv:1602.07576 (Feb. 2016), arXiv:1602.07576. arXiv: 1602.07576 [cs.LG].
- [45] Husni Almoubayyed, Rachel Mandelbaum, Humna Awan, Eric Gawiser, R. Lynne Jones, Joshua Meyers, J. Anthony Tyson, Peter Yoachim, and The LSST Dark Energy Science Collaboration. “Optimizing LSST observing strategy for weak lensing systematics”. In: *Monthly Notices of the Royal Astronomical Society* 499.1 (Nov. 2020), pp. 1140–1158. arXiv: 2006.12538 [astro-ph.CO].
- [46] Alan Junzhe Zhou, Xiangchong Li, Scott Dodelson, and Rachel Mandelbaum. “Accurate field-level weak lensing inference for precision cosmology”. In: *Physical Review D* 110.2, 023539 (July 2024), p. 023539. arXiv: 2312.08934 [astro-ph.CO].
- [47] A. Loureiro, L. Whiteway, E. Sellentin, J. S. Lefaurie, A. H. Jaffe, and A. F. Heavens. “Almanac: Weak Lensing power spectra and map inference on the masked sphere”. In: *The Open Journal of Astrophysics* 6, 6 (Feb. 2023), p. 6. arXiv: 2210.13260 [astro-ph.CO].
- [48] Supranta S. Boruah, Eduardo Rozo, and Pier Fiedorowicz. “Map-based cosmology inference with lognormal cosmic shear maps”. In: *Monthly Notices of the Royal Astronomical Society* 516.3 (Oct. 2022), pp. 4111–4122. arXiv: 2204.13216 [astro-ph.CO].
- [49] Pier Fiedorowicz, Eduardo Rozo, Supranta S. Boruah, Chihway Chang, and Marco Gatti. “KaRMMa – Kappa Reconstruction for Mass Mapping”. In: *Monthly Notices of the Royal Astronomical Society* 512.1 (Mar. 2022), pp. 73–85. arXiv: 2105.14699 [astro-ph.CO].
-

-
- [50] Natalia Porqueres, Alan Heavens, Daniel Mortlock, Guilhem Lavaux, and T. Lucas Makinen. “Field-level inference of cosmic shear with intrinsic alignments and baryons”. In: *arXiv e-prints* (Apr. 2023). arXiv: 2304.04785 [astro-ph.CO].
- [51] H. T. Jense, I. Harrison, E. Calabrese, A. Spurio Mancini, B. Bolliet, J. Dunkley, and J. C. Hill. “A complete framework for cosmological emulation and inference with CosmoPower”. In: *RAS Techniques and Instruments* 4, rzaf002 (2025), rzaf002. arXiv: 2405.07903 [astro-ph.CO].
- [52] Davide Piras and Alessio Spurio Mancini. “CosmoPower-JAX: high-dimensional Bayesian inference with differentiable cosmological emulators”. In: *The Open Journal of Astrophysics* 6, 20 (2023), p. 20. arXiv: 2305.06347 [astro-ph.CO].
- [53] Divij Sharma, Biwei Dai, Francisco Villaescusa-Navarro, and Uroš Seljak. “A field-level emulator for modelling baryonic effects across hydrodynamic simulations”. In: *Monthly Notices of the Royal Astronomical Society* 538 (2025), p. 1415. arXiv: 2401.15891 [astro-ph.CO].
- [54] Tianhuan Lu, Zoltán Haiman, and Xiangchong Li. “Cosmological constraints from HSC survey first-year data using deep learning”. In: *Monthly Notices of the Royal Astronomical Society* 521.2 (2023), p. 2050. arXiv: 2301.01354 [astro-ph.CO].
- [55] M. Gatti, G. Campailla, N. Jeffrey, L. Whiteway, A. Porredon, J. Prat, J. Williamson, M. Raveri, B. Jain, V. Ajani, et al. “Dark Energy Survey Year 3 results: Simulation-based cosmological inference with wavelet harmonics, scattering transforms, and moments of weak lensing mass maps. II. Cosmological results”. In: *Physical Review D* 111.6, 063504 (2025), p. 063504. arXiv: 2405.10881 [astro-ph.CO].
- [56] Biwei Dai and Uros Seljak. “Multiscale Flow for Robust and Optimal Cosmological Analysis”. In: *Machine Learning for Astrophysics*. 2023, 10, p. 10. arXiv: 2306.04689 [astro-ph.CO].
- [57] Ioannis Pantos and Leandros Perivolaropoulos. “Status of the S_8 tension: A 2026 review of probe discrepancies”. In: *Phys. Dark Universe* 52, 102286 (June 2026), p. 102286. arXiv: 2602.12238 [astro-ph.CO].
- [58] E. E. Falco, M. V. Gorenstein, and I. I. Shapiro. “On model-dependent bounds on H_0 from gravitational images : application to Q 0957+561 A, B.” In: *ApJ* 289 (Feb. 1985), pp. L1–L4.
- [59] Kenneth C. Wong, Sherry H. Suyu, Geoff C.-F. Chen, Cristian E. Rusu, Martin Millon, et al. “H0LiCOW - XIII. A 2.4 per cent measurement of H_0 from lensed quasars: 5.3σ tension between early- and late-Universe probes”. In: *MNRAS* 498.1 (Oct. 2020), pp. 1420–1439. arXiv: 1907.04869 [astro-ph.CO].
- [60] S. Birrer, A. J. Shajib, A. Galan, M. Millon, T. Treu, et al. “TDCOSMO. IV. Hierarchical time-delay cosmography - joint inference of the Hubble constant and galaxy density profiles”. In: *A&A* 643, A165 (Nov. 2020), A165. arXiv: 2007.02941 [astro-ph.CO].
- [61] Anowar J. Shajib, Graham P. Smith, Simon Birrer, Aprajita Verma, Nikki Arendse, Thomas Collett, Tansu Daylan, Stephen Serjeant, and LSST Strong Lensing Science Collaboration. “Strong gravitational lenses from the Vera C. Rubin Observatory”. In: *Philosophical Transactions of the Royal Society of London Series A* 383.2295, 20240117 (May 2025), p. 20240117. arXiv: 2406.08919 [astro-ph.CO].
- [62] Narayan Khadka, Simon Birrer, Alexie Leauthaud, and Holden Nix. “Breaking the mass-sheet degeneracy in strong lensing mass modelling with weak lensing observations”. In: *MNRAS* 533.1 (Sept. 2024), pp. 795–806. arXiv: 2404.01513 [astro-ph.CO].
- [63] Siddharth Mishra-Sharma, David Alonso, and Joanna Dunkley. “Neutrino masses and beyond- Λ CDM cosmology with LSST and future CMB experiments”. In: *Physical Review D* 97.12, 123544 (2018), p. 123544. arXiv: 1803.07561 [astro-ph.CO].
-

-
- [64] [Xiangchong Li](#), Nobuhiko Katayama, Masamune Oguri, and Surhud More. “Fourier Power Function Shapelets (FPFS) shear estimator: performance on image simulations”. In: MNRAS 481.4 (Dec. 2018), pp. 4445–4460. arXiv: [1805.08514](#) [[astro-ph.CO](#)].
- [65] Colin J. Burke, Patrick D. Aleo, Yu-Ching Chen, Xin Liu, John R. Peterson, et al. “Deblending and classifying astronomical sources with Mask R-CNN deep learning”. In: MNRAS 490.3 (Dec. 2019), pp. 3952–3965. arXiv: [1908.02748](#) [[astro-ph.IM](#)].
- [66] Grant Merz, Yichen Liu, Colin J. Burke, Patrick D. Aleo, Xin Liu, et al. “Detection, instance segmentation, and classification for astronomical surveys with deep learning (DEEPDISC): DETECTOR2 implementation and demonstration with Hyper Suprime-Cam data”. In: MNRAS 526.1 (Nov. 2023), pp. 1122–1137. arXiv: [2307.05826](#) [[astro-ph.IM](#)].
- [67] Grant Merz, Xin Liu, Samuel Schmidt, Alex I. Malz, Tianqing Zhang, et al. “DeepDISC-photoz: Deep Learning-Based Photometric Redshift Estimation for Rubin LSST”. In: *The Open Journal of Astrophysics* 8, 40 (Apr. 2025), p. 40. arXiv: [2411.18769](#) [[astro-ph.IM](#)].
- [68] The AION Collaboration et al. “AION-1: Omnimodal Foundation Model for Astronomical Sciences”. In: *arXiv e-prints*, arXiv:2510.17960 (Oct. 2025), arXiv:2510.17960. arXiv: [2510.17960](#) [[astro-ph.IM](#)].
- [69] Sudeep Das, Roland de Putter, Eric V. Linder, and Reiko Nakajima. “Weak Lensing Science, Surveys, and Systematics”. In: *J. Cosmology Astropart. Phys.* 2012.11 (Nov. 2012), p. 011. arXiv: [1102.5090](#) [[astro-ph.CO](#)].
- [70] LSST Dark Energy Science Collaboration, Bela Abolfathi, et al. “The LSST DESC DC2 Simulated Sky Survey”. In: ApJS 253.1, 31 (Mar. 2021), p. 31. arXiv: [2010.05926](#) [[astro-ph.IM](#)].
- [71] M. A. Troxel, C. Lin, A. Park, C. Hirata, R. Mandelbaum, et al. “A joint Roman Space Telescope and Rubin Observatory synthetic wide-field imaging survey”. In: MNRAS 522.2 (June 2023), pp. 2801–2820. arXiv: [2209.06829](#) [[astro-ph.IM](#)].
- [72] OpenUniverse, The LSST Dark Energy Science Collaboration, The Roman HLIS Project Infrastructure Team, The Roman RAPID Project Infrastructure Team, The Roman Supernova Cosmology Project Infrastructure Team, et al. “OpenUniverse2024: a shared, simulated view of the sky for the next generation of cosmological surveys”. In: MNRAS 544.4 (Dec. 2025), pp. 3799–3823. arXiv: [2501.05632](#) [[astro-ph.CO](#)].
- [73] J. Prat et al. “The catalog-to-cosmology framework for weak lensing and galaxy clustering for LSST”. In: *The Open Journal of Astrophysics* 6, 13 (May 2023), p. 13. arXiv: [2212.09345](#) [[astro-ph.CO](#)].
- [74] [Xiangchong Li](#), Hironao Miyatake, Wentao Luo, Surhud More, Masamune Oguri, et al. “The three-year shear catalog of the Subaru Hyper Suprime-Cam SSP Survey”. In: PASJ 74.2 (Apr. 2022), pp. 421–459. arXiv: [2107.00136](#) [[astro-ph.CO](#)].
- [75] [Xiangchong Li](#), Tianqing Zhang, Sunao Sugiyama, Roohi Dalal, Ryo Terasawa, et al. “Hyper Suprime-Cam Year 3 results: Cosmology from cosmic shear two-point correlation functions”. In: Phys. Rev. D 108.12, 123518 (Dec. 2023), p. 123518. arXiv: [2304.00702](#) [[astro-ph.CO](#)].
- [76] Roohi Dalal, [Xiangchong Li](#), Andrina Nicola, Joe Zuntz, Michael A. Strauss, et al. “Hyper Suprime-Cam Year 3 results: Cosmology from cosmic shear power spectra”. In: Phys. Rev. D 108.12, 123519 (Dec. 2023), p. 123519. arXiv: [2304.00701](#) [[astro-ph.CO](#)].
- [77] Tianqing Zhang, [Xiangchong Li](#), Sunao Sugiyama, Rachel Mandelbaum, Surhud More, et al. “Cosmology and Source Redshift Constraints from Galaxy Clustering and Tomographic Weak Lensing with HSC Y3 and SDSS using the Point-Mass Correction Model”. In: *arXiv e-prints*, arXiv:2507.01386 (July 2025), arXiv:2507.01386. arXiv: [2507.01386](#) [[astro-ph.CO](#)].
-

APPENDIX 2: Facilities & Other Resources

The proposed work will be carried out at Brookhaven National Laboratory (BNL), drawing on two federally supported computing facilities and on the PI's standing data-access rights to Rubin LSST and Euclid imaging.

2.1 BNL Scientific Data and Computing Center (SDCC)

The BNL Scientific Data and Computing Center (SDCC) provides the institutional high-throughput computing and storage backbone for the proposed work. SDCC operates a moderate-scale CPU/GPU batch cluster and multi-petabyte storage. SDCC's storage capacity will host public Euclid data products at BNL, providing low-latency local access to Euclid imaging for the joint LSST×Euclid image-processing pipeline. SDCC will be used primarily for pipeline development, continuous-integration testing against `descwl-shear-sims` / `LSST imSim`, and small-to-medium production runs of the joint pipeline.

2.2 National Energy Research Scientific Computing Center (NERSC)

As a member of the LSST DESC, the PI and any researchers working with the PI have access to the LSST DESC computing allocation at the National Energy Research Scientific Computing Center (NERSC), renewed annually through the DOE ERCAP process. NERSC's Perlmutter system—with NVIDIA A100 Tensor Core GPU nodes (over 6,000 GPUs in aggregate) and capable parallel scratch file systems—is well-matched to the GPU-accelerated image-simulation campaigns, AI-based shear-measurement training runs, and joint-imaging shear-catalog production proposed here. The forthcoming NERSC-10 (Doudna) system, scheduled to enter production during the proposal period, will further accelerate the AI-extension and field-level-inference workloads. NERSC's large global file systems additionally provide a natural shared workspace for distributing the resulting image-simulation suites, joint shear catalogs, and photo-*z* training sets across the LSST DESC collaboration.

2.3 Data Access

As a U.S. institution, BNL receives full data rights to Rubin Observatory data products through and beyond LSST DR1 and DR2. The PI is a pipeline scientist within the LSST DESC, with full access to DESC-internal data products including the LSST DP1 and DP2 AnaCal shear catalogs the PI produces. Access to Euclid imaging is obtained through Euclid's planned public releases (Quick Release Q2, DR1 in October 2026, DR2 in March 2029), in coordination with the LSST DESC–Euclid Consortium joint analysis working groups.

APPENDIX 3: Equipment

No specialized new equipment is required for the proposed research. All computational work will be carried out on the SDCC and NERSC facilities described in Appendix 2; no additional hardware purchase, leasing, or installation is proposed.

APPENDIX 4: Data Management Plan

This proposal adopts the LSST DESC Data Management Plan¹ in full, with the additions described below.

4.1 Data Types and Sources

The proposed work will produce: (i) overlapping ground–space image simulations of the Rubin Deep Drilling Fields and overlapping Euclid/Roman deep fields; (ii) joint LSST×Euclid shear catalogs and the corresponding analytical shear-response calibration products; (iii) joint LSST+Euclid photometric-redshift catalogs and trained estimators; (iv) Gaussian-prior field-level cosmology posterior samples and likelihoods; and (v) software packages implementing the joint pipeline and the field-level inference backbone.

4.2 Data Content, Format, and Preservation

All catalog products will be stored in standard astronomical formats (FITS, HDF5, Parquet) and curated within the LSST DESC data infrastructure at NERSC, with redundant copies at BNL SDCC. Image simulations are produced from version-controlled configurations released alongside the data. Posterior samples and trained AI estimators are distributed in HDF5 with accompanying metadata describing model configuration, training data, and validation results.

4.3 Sharing and Open-Source Release

Publications resulting from this proposal will be submitted to peer-reviewed journals and simultaneously posted to arXiv. Data underlying each publication’s figures will be released to a Zenodo repository under a CC-BY license upon acceptance of the corresponding paper. Software developed under this program—AnaCal and its joint-imaging extension, the joint photo- z pipeline, and the field-level inference backbone—will be released on GitHub under permissive open-source licenses (MIT/BSD), following standard LSST DESC release-engineering practice and the PI’s existing AnaCal practice (semantic versioning, continuous integration, archival snapshots on Zenodo).

¹https://lsstdesc.org/assets/pdf/docs/DESC_DMP_latest.pdf

APPENDIX 5: Synergistic Activities

1. **Pipeline scientist within the LSST Dark Energy Science Collaboration (DESC):** the PI produced the LSST Data Preview 1 AnaCal shear catalog and is currently leading the LSST Data Preview 2 AnaCal shear catalog for collaboration-wide use.
2. **Convener of the HSC weak-lensing working group:** the PI coordinates the Subaru Hyper Suprime-Cam (HSC) weak-lensing analysis effort, led the HSC Year-3 image-simulation campaign and shear catalog and the corresponding cosmic-shear cosmology analyses, and is leading the ongoing HSC Year-6 shear catalog.
3. **Mentoring and training students in DESC:** the PI co-supervises graduate students extending AnaCal to AI-based shear estimators and contributed to the supervision of the graduate student who developed the Miko field-level WL inference pipeline.
4. **Referee for major astronomy and astrophysics journals:** the PI serves as a referee for leading journals in the field, including *The Astrophysical Journal* (ApJ), *Monthly Notices of the Royal Astronomical Society* (MNRAS), *Astronomy & Astrophysics* (A&A), and *The Open Journal of Astrophysics* (OJA), contributing to peer review of weak-lensing, cosmology, and survey-methodology manuscripts.
5. **Organizer of the BNL Particle Physics seminar:** the PI organizes the Brookhaven National Laboratory Particle Physics seminar series,² hosting external speakers and fostering exchange between the experimental, theoretical, and cosmology programs across the laboratory.

²<https://indico.bnl.gov/category/134/>

APPENDIX 6: Transparency of Foreign Connections

Not applicable.

APPENDIX 7: Other Attachments

Not applicable.